

280-420 GHz Single Ended Rx ('Barney')

Jacob Kooi, Chip Sumner, Riley Ceria

March 12, 2006

Attached is some information about the new tunerless 345 GHz receiver, nicknamed 'Barney'. Barney has now been installed at the CSO, and aside from a focus curve and pointing file it should be ready for action. Hold time on the dewar appears to be 24.5 hours. As you will see in the following plots, the response is quite spectacular. A great deal of time has been spent on minimizing optics loss, which clearly has paid off. Another important feature of 'Barney' is that of remote tuning, stability, and the avoidance of ground loops. The latter is evident in the nice performance on the telescope. Finally, we have successfully measured the beam position and illumination on the secondary (CSO) mirror.

I. FTS Measurements (David Miller, Jacob Kooi)

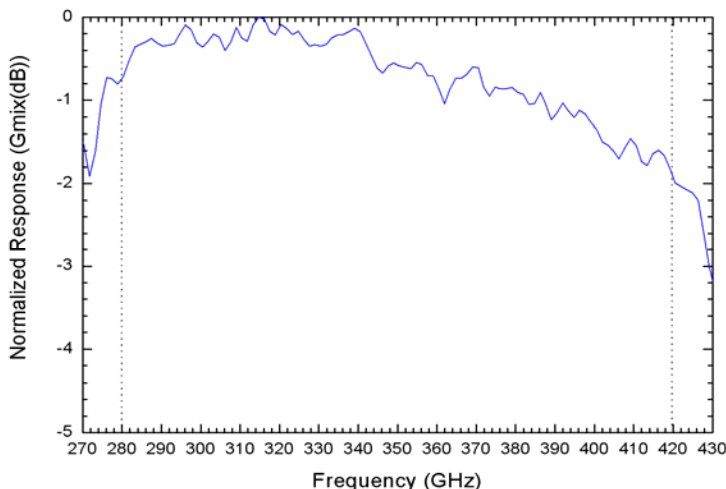


Fig. 1 Direct detection FTS measurement at Caltech

II. Calculated Sideband Ratio

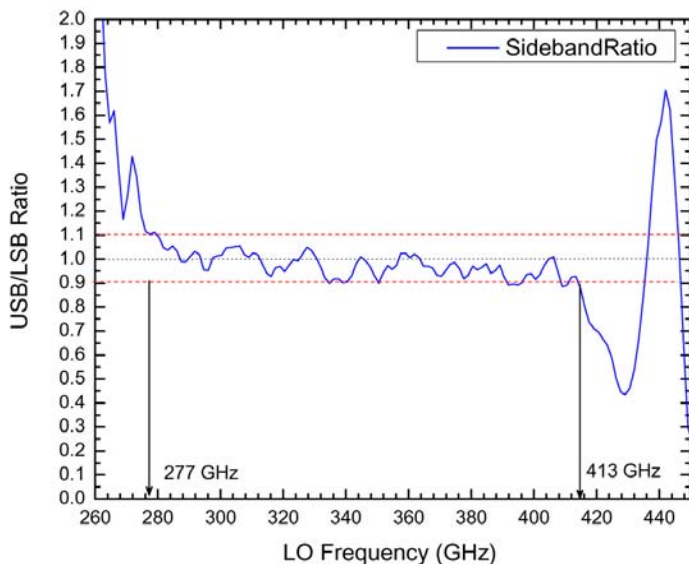


Fig. 2 Derived Sideband Ratio from FTS Measurement

III. Heterodyne Receiver Noise Temperature

A great deal of time has been spent on automating the data acquisition system. This was deemed particular important as a demonstration of remote receiver operation. Remote control of the receiver has enabled us to take multiple Megabytes of characterization data. Having this capability has been an tremendous aid in understanding the instrument. We find that the bias conditions of ‘Barney’ are very stable and predictable across the frequency range. They are:

V_{sis}: 2-2.15 mV, I_{sis}: 85-90uA, B-field: 30-33 mA

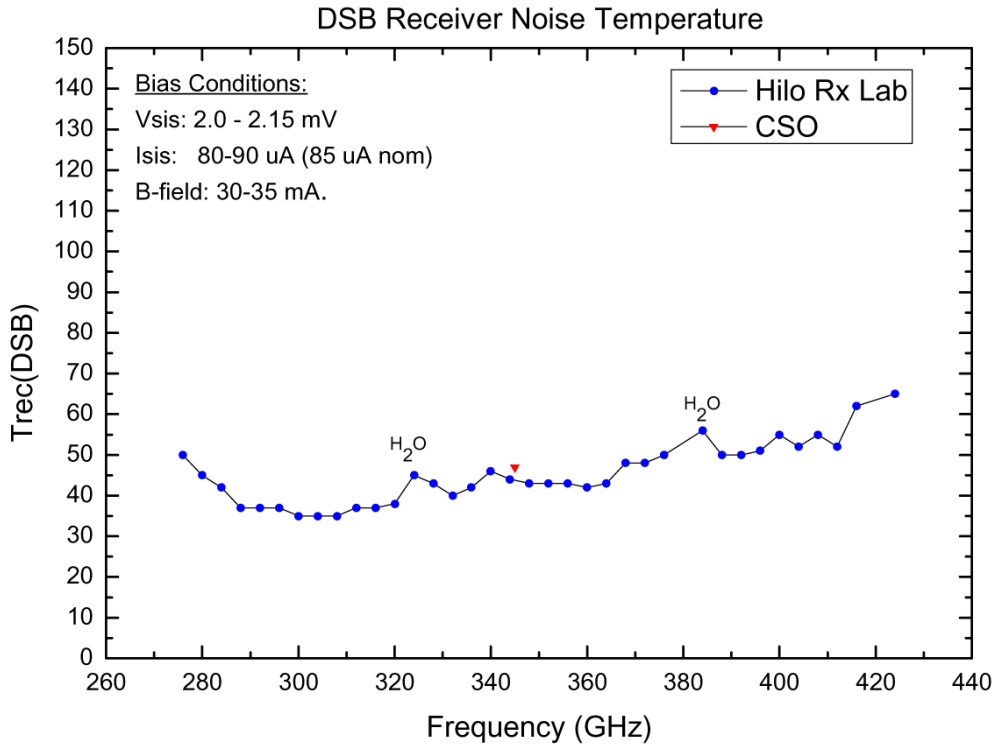


Fig. 3. Measured receiver noise temperature in the Hilo receiver lab (blue) and at the CSO (red) as a confirmation.

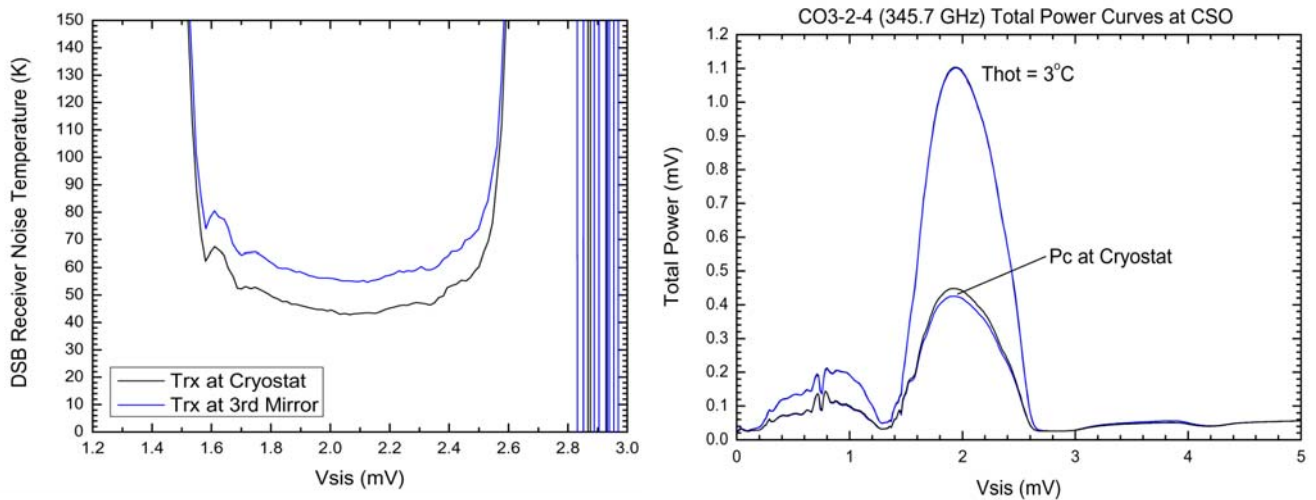


Fig. 4. Receiver Noise temperature as measured on the relay optics at the cryostat and 3rd CSO mirror.

IV. 345 GHz B-field Characterization

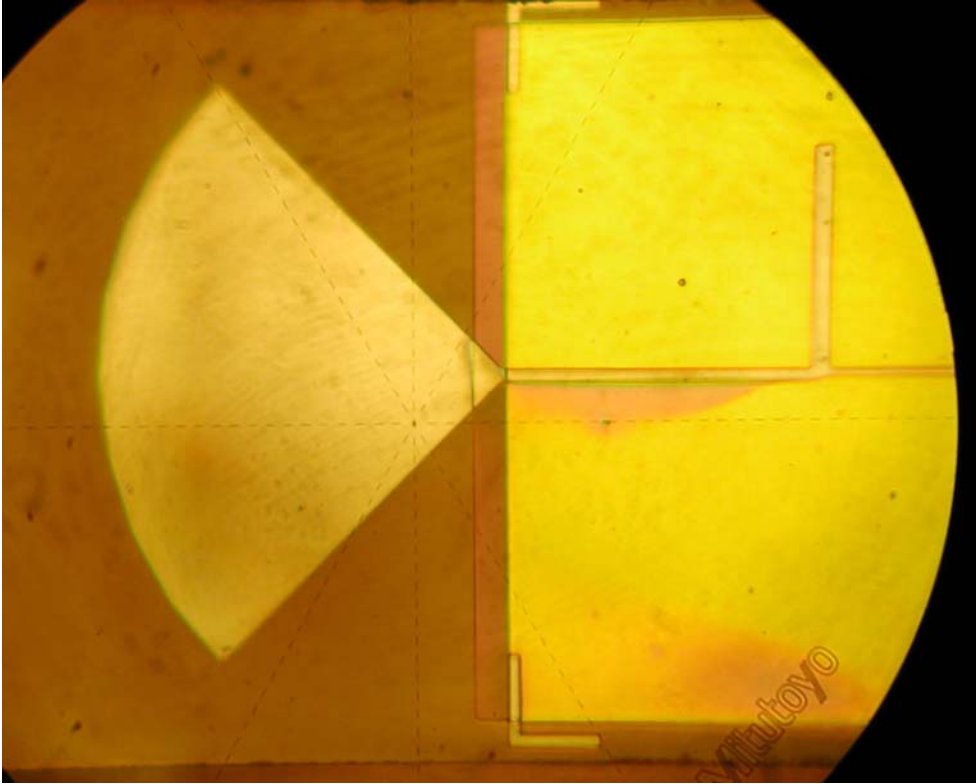


Fig. 5. Two high current density ($RnA=7.6$) twin junctions configured in parallel are used to achieve the broad RF performance. We find that there is an odd interaction between the two junctions that may be suppressed by magnetic field. It appears not related to the breaking of Cooper pairs, as the Josephson effect is already completely suppressed with 15mA of magnet field current. Rather some sort of circuit induced (Squid?) interaction seems likely. It certainly makes for interesting physics. Applying a magnet current of 30 mA appears adequate to squelch the effect. Of course with an enhanced magnetic field the gap is reduced and mixer gain is reduced. This is demonstrated in Fig. 5. We have taken similar data at 280, 316, 384 and 424 GHz and the behavior is very similar. Increasing the B-field > 30 mA seems to have no other effect than reducing then mixer gain and lowering then noise.

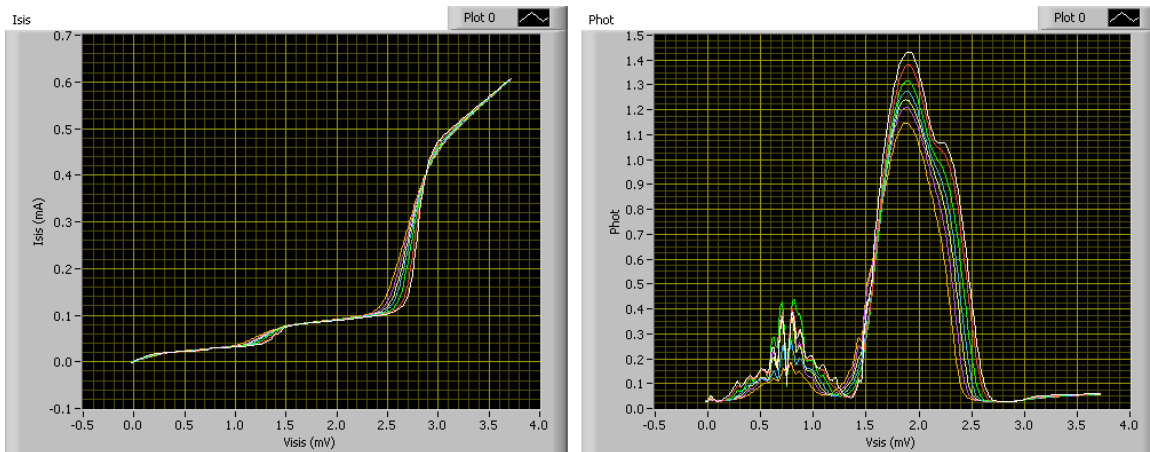


Fig. 6. Effect of applying a large magnetic field on the superconducting gap and mixer conversion gain. . Magnet Field current: 16.3, 20, 25, 30, 35, 40, 50 mA,

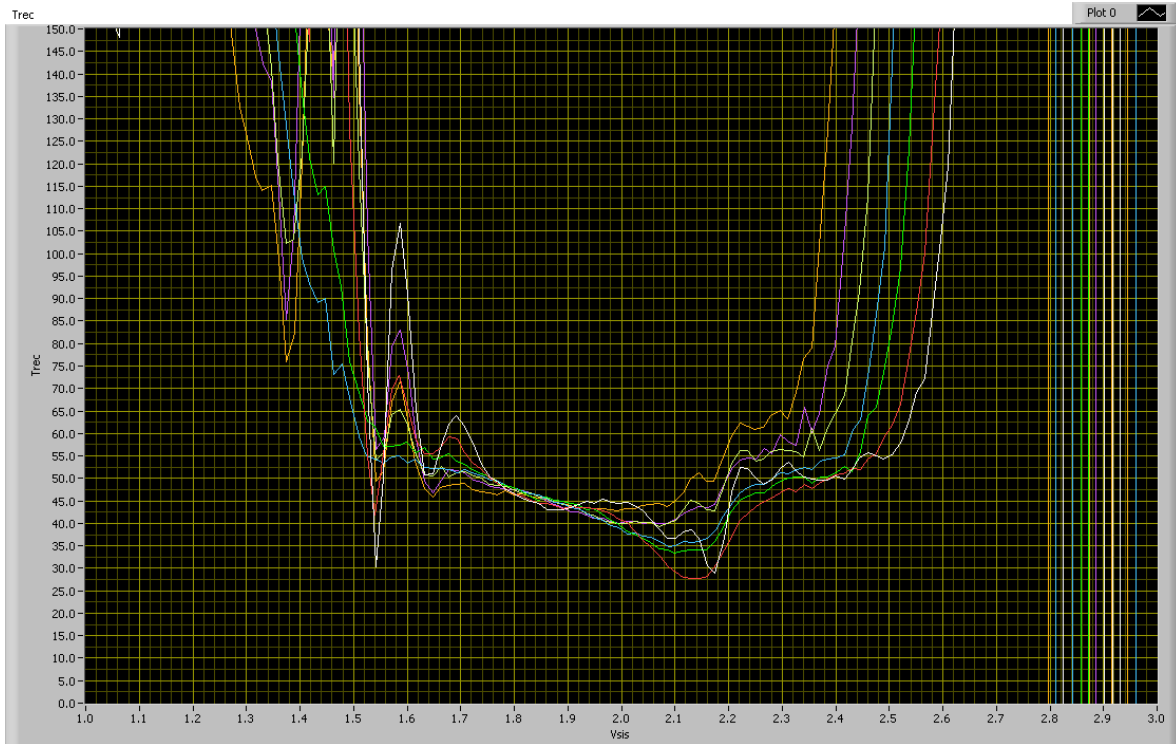


Fig. 7. Effect of applying a large magnetic field on the Receiver noise temperature. Starting at the right (white curve) the Josephson effect is properly nulled with 16.3 mA of magnet field current. This however gives a wildly fluctuating, and therefore not very realistic receiver noise temperature. As the magnetic field current is increased the receiver noise temperature wiggles disappear. This behavior is observed throughout the entire 280-420 GHz band, with the position of the wiggles having a frequency dependence. At 280 GHz the wiggles are at low bias (1.8 mV) whereas at 420 GHz they appear at 2.4 mV. At the center frequency they appear in the middle of the photon step. This effect is presumably related to some kind of squid/microstrip interaction Magnet Field current: 16.3 (white) , 20, 25, 30, 35, 40, 50 mA (yellow)

V. 345 GHz SIS Current Characterization

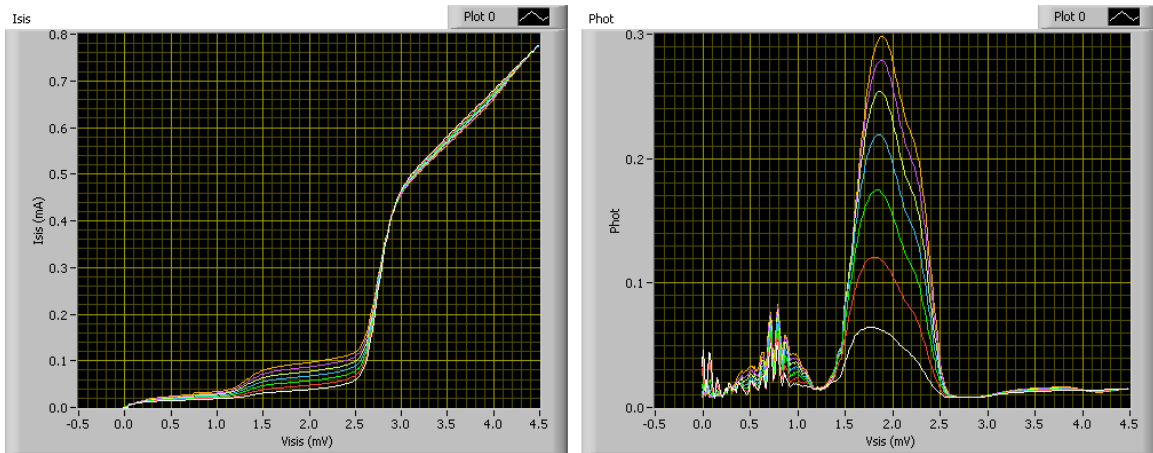


Fig. 8 I_{SIS} : 40(white), 50, 60, 70, 80, 90 100 uA (yellow).. Optimal Bias current 80-90 uA. ($T_{rec} \sim 42K$ DSB from 2.0 – 2.15 mV). B-field current set to $\sim 30mA$. With increased SIS Pump current (alpha) the mixer gain increases (right curve).

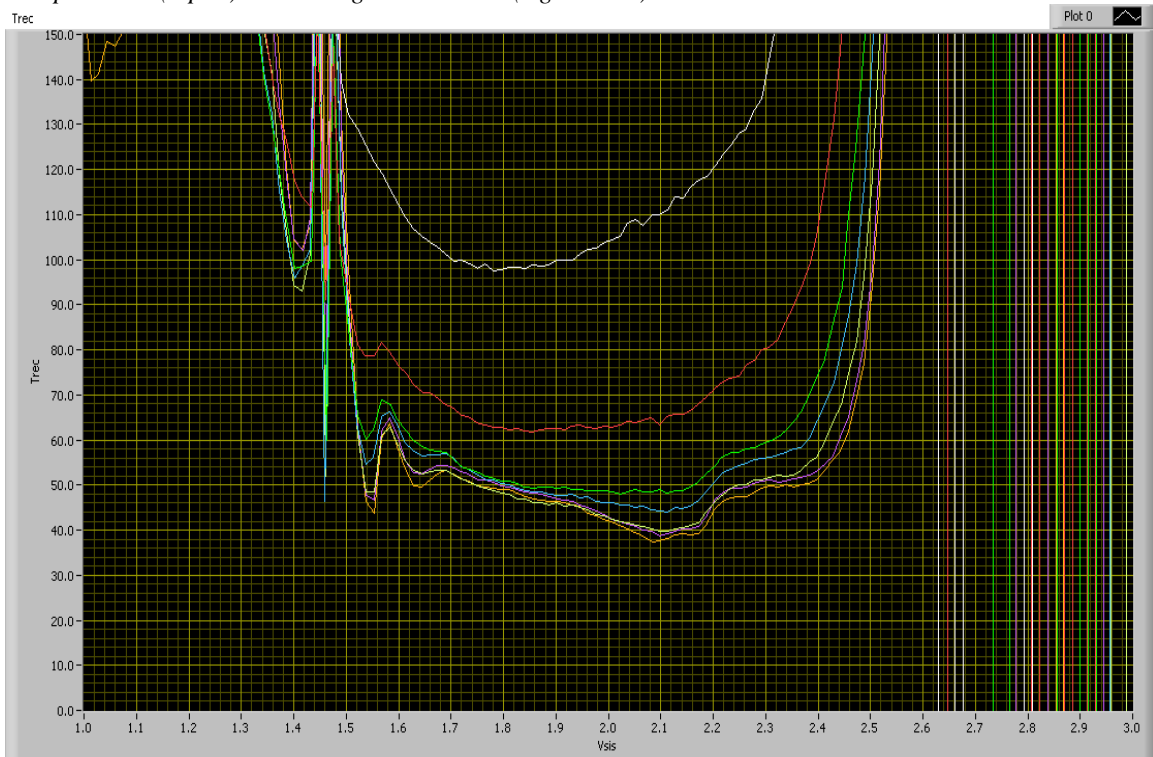


Fig. 9 I_{SIS} : 40(white), 50, 60, 70, 80, 90 100 uA (yellow).. Optimal Bias current 80-90 uA. ($T_{rec} \sim 42K$ DSB from 2.0 – 2.15 mV). B-field current set to $\sim 30mA$.

V. 296 GHz Receiver Noise Temperature

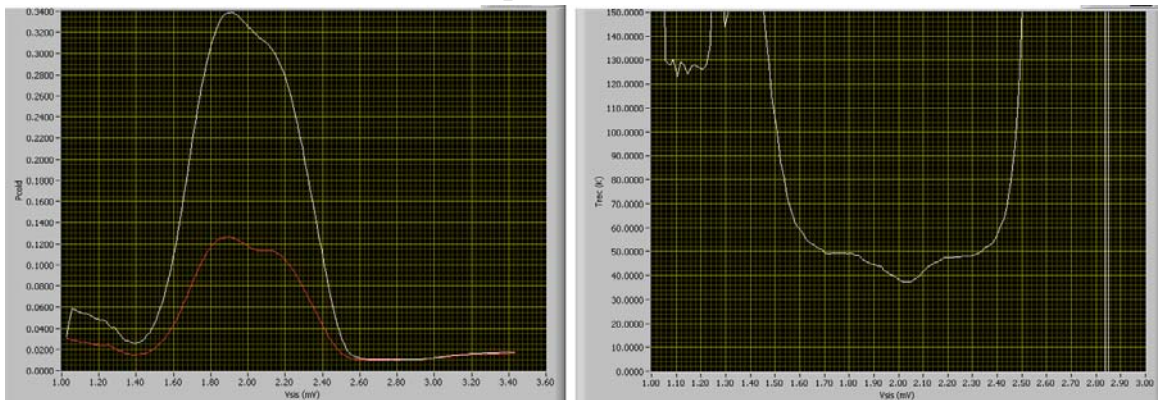


Fig. 10 DSB Receiver noise temperature for $I_{is} = 85 \mu A$.at 296 GHz. B-field current set to 32.8 mA.

VI. 348 GHz Receiver Noise Temperature

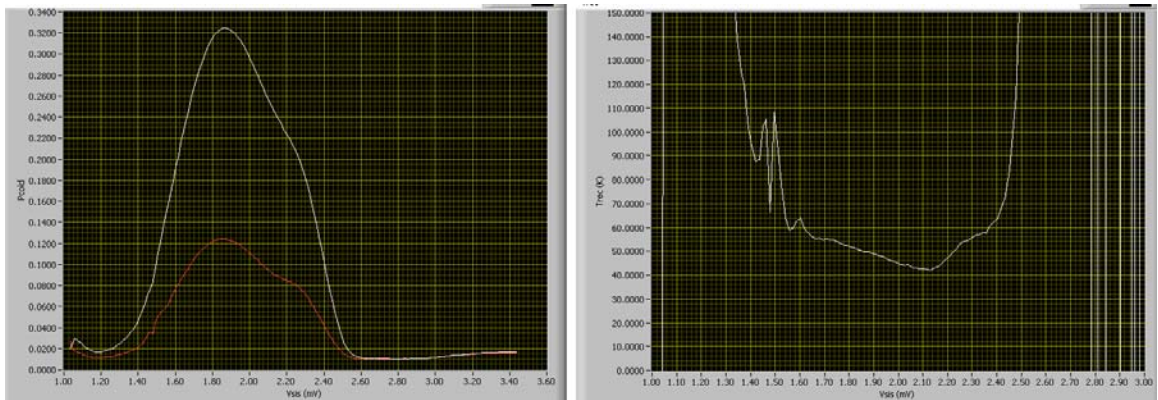


Fig. 11 DSB Receiver noise temperature for $I_{is} = 85 \mu A$.at 348GHz. B-field current set to 33 mA.

VII. 416 GHz Receiver Noise Temperature

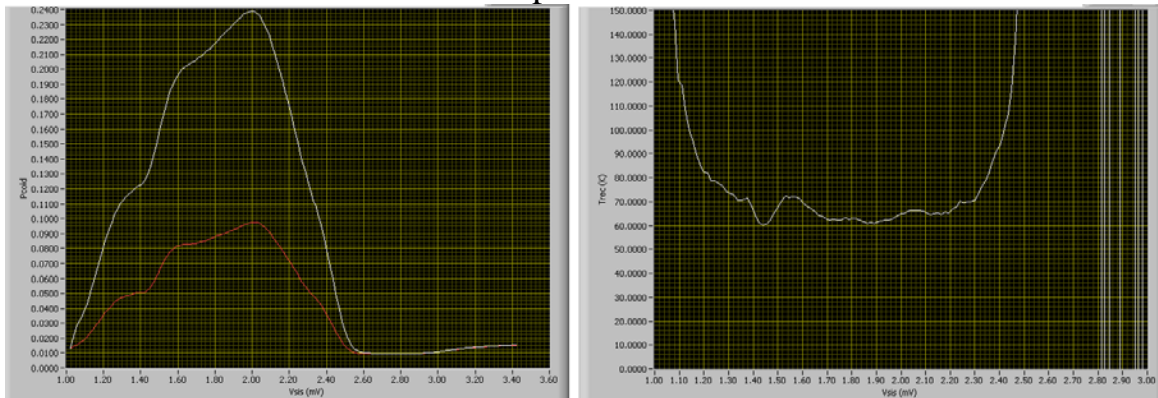


Fig. 12 DSB Receiver noise temperature for $I_{is} = 85 \mu A$.at 416 GHz. B-field current set to 31.4 mA.

IV. Receiver Stability at the CSO

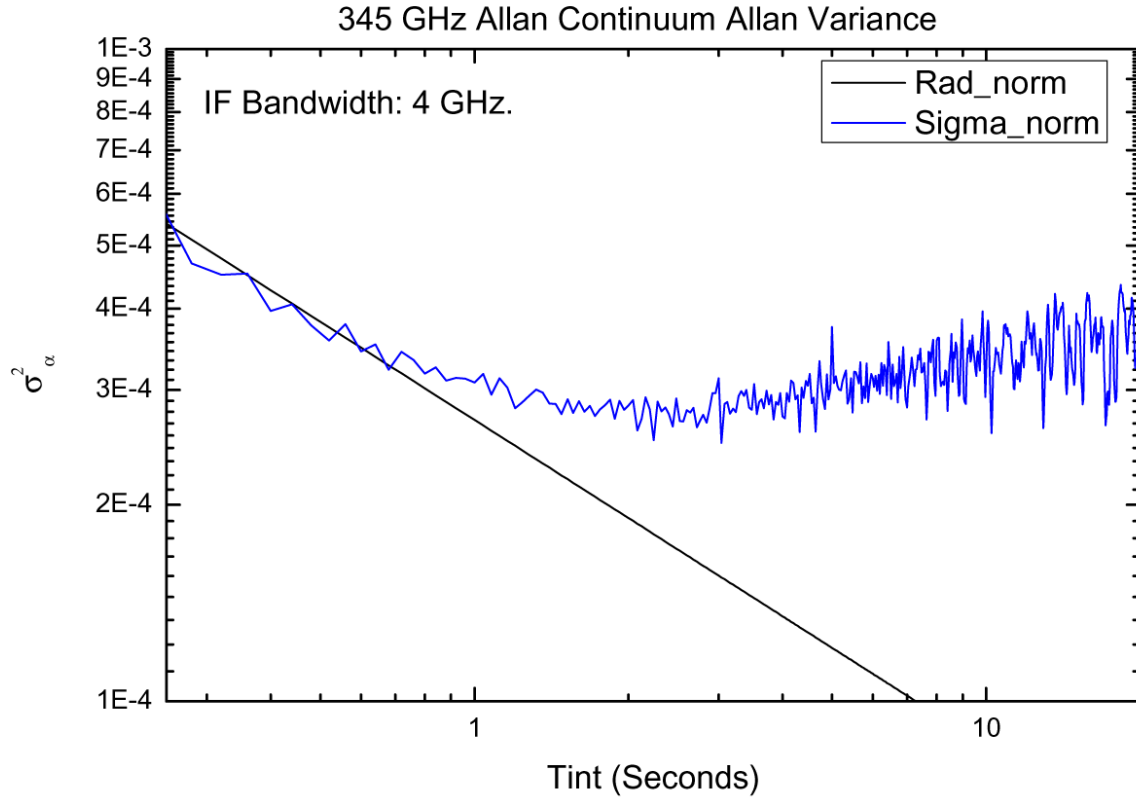


Fig. 13. Allan variance of the entire 4 GHz (continuum) IF with ‘Barney’ mounted at on the relay-optics. The receiver looks onto a 296K eccosorb blackbody on the 4th relay-optics mirror. At approximately 0.8 second the curve begins to deviate from the ideal radiometer equation. The Allan minimum time occurs at approximately 2 seconds. This means that for 4 GHz continuum measurements at a secondary chop frequency of 1 Hz is adequate. Since the stability scales with approximately the root (BW), we estimate a stability of 48 seconds in a 1.5 MHz spectrometer noise bandwidth. The instrument stability is thus likely limited by the sky. Finally, the horizontal behavior is indicative of gain fluctuation noise due to for example bias noise on then SIS, LNA, and Total Power box.

IV. CSO Secondary Beam Measurements

The beam is centered on the 5th and 4th relay optics mirror. It is however offset from center by 1.5 inches on the 3rd mirror (sideways ok, up toward control room). On the 2nd the alignment is good up/down, but it is 1.25" off sideways (toward the machine shop). Design goal for the secondary edgetaper is 11dB at 345 GHz. The difference between design and measurement is likely due to 4.4mm (175 mils) cold stage contraction of the cryostat. This has not been taken into account in the optical calculations. **If so desired, then four mounting legs of Barney may be machined of by 0.175 Inches.** Note that a frequency independent design is only possible with the addition of a second focusing element in the receiver. This was deemed unnecessary (Fig. 18)

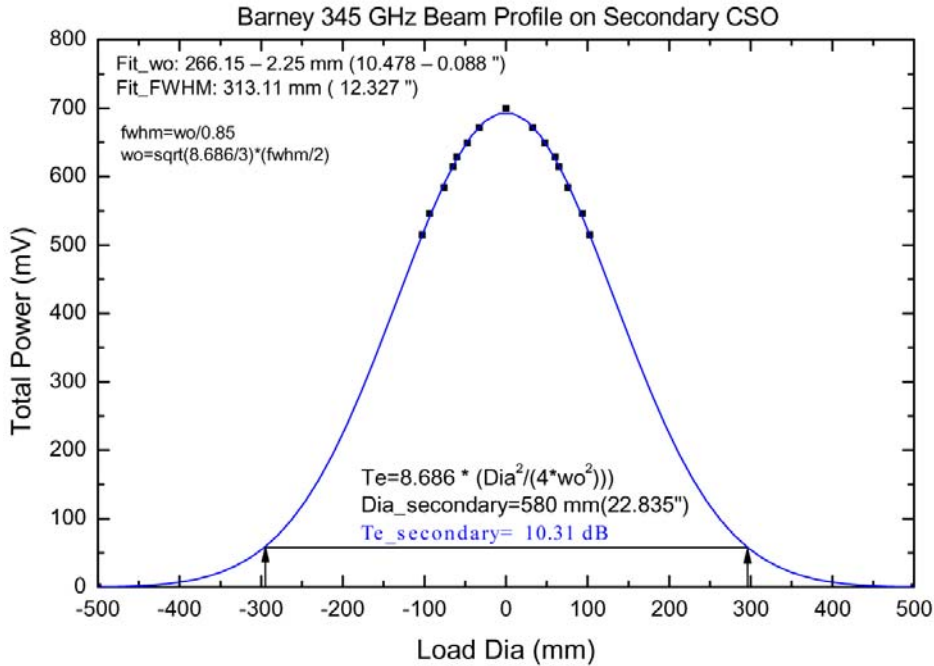


Fig. 14 Beam Profile on the Secondary. Edgetaper is 10.31 dB (11dB design goal).

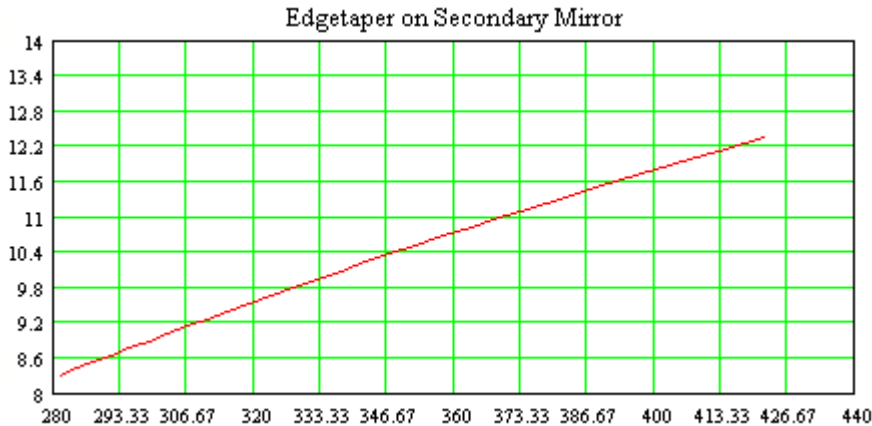


Fig. 15 Edgetaper on the secondary. At 345 GHz the taper is 10.31 dB (11dB design goal). The discrepancy between theory and measurement is due to a 4.4mm uncounted shrinkage of the dewar. Shimming 0.175" of the mounting legs of Barney will correct the situation, though actual performance gain looks minimal (Fig.'s 17-18)

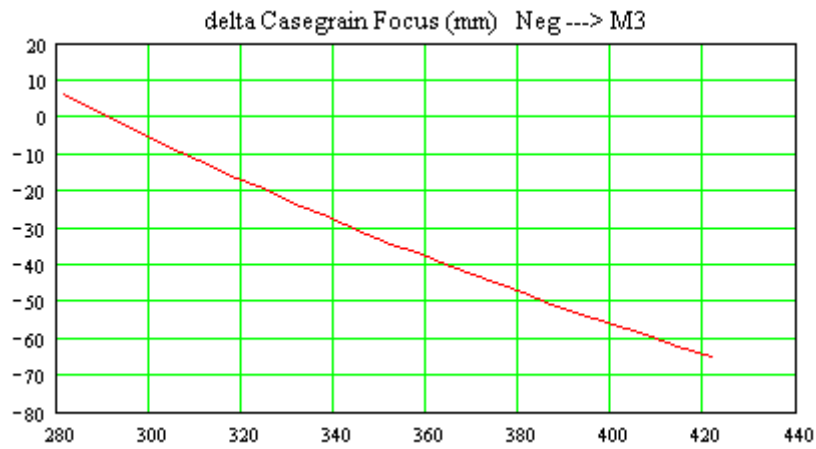


Fig. 16. Focus Offset as a function of Frequency based on a 10.31 dB Taper. At 345 GHz the focus offset is 30mm towards M3. If the feed legs of the cryostat are trimmed then nominal focus will shift back to 350 GHz.

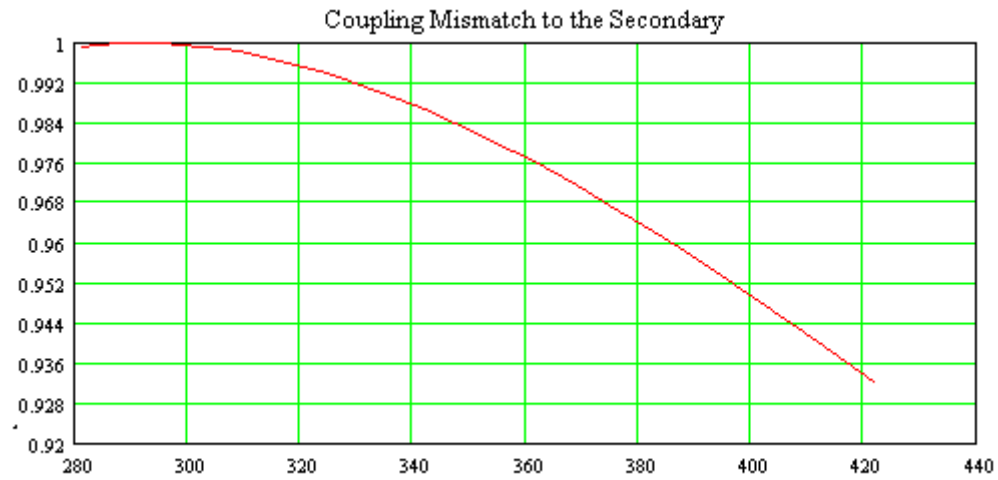


Fig. 17. Coupling Mismatch when then focus is set to nominal.

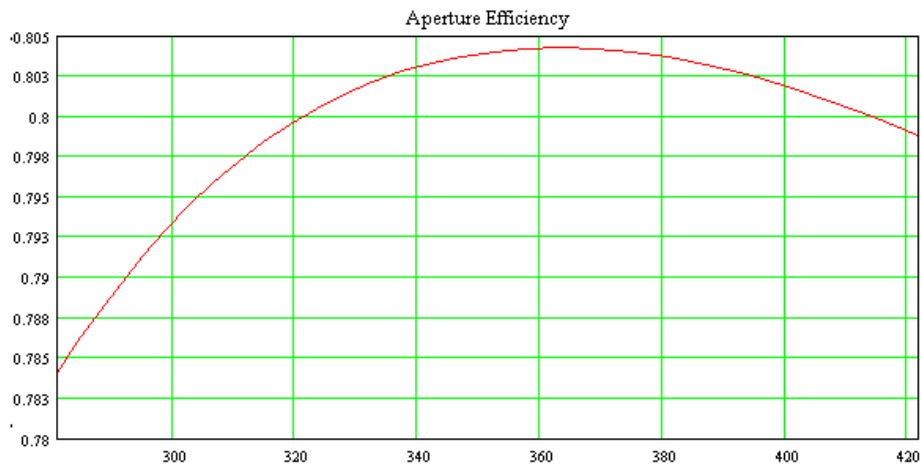


Fig. 18. Aperture Efficiency based on the measured 10.31dB Taper at 345 GHz.

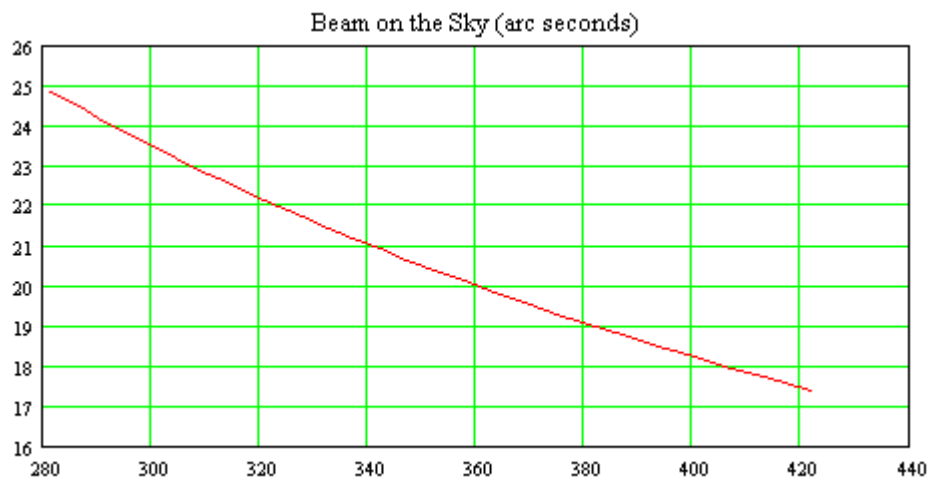


Fig. 19. FWHM Sky Beam